Thermal fatigue evaluation of partially cooled pipes

Nobuchika Kawasaki[1)], Hideki Takasho[2)], Naoto Kasahara[1)]

1) O-arai Engineering Center, Japan Nuclear Cycle Development Institute,
2) Joyo Industries Ltd.

30th MPA-Seminar in conjunction with the 9th German-Japanese Seminar
Stuttgart, October 6 and 7, 2004

Abstract

Concerning thermal striping phenomenon with a cold/hot spot, effect of the thermal spot on fatigue strength was investigated. The thermal spot causes membrane stress and enhances bending stress in the structure. Increased stress shortens the fatigue life and accelerates the crack propagation rate. The mechanism to increase stress was found to be the structural constraint of thermal strain by the thermal spot. To consider this mechanism, constraint efficiency factors were introduced to the thermal stress evaluation method based on frequency transfer functions developed by authors. Proposed method with these factors was validated through comparisons with cyclic FEA considering thermal spots.

Nomenclature

T_f, $T_f^* = T_f / T_0$: Fluid temperature
T_s, $T_s^* = T_s / T_0$: Structural temperature
R_m, R_b: Constraint efficiency factors
$Bi = hL/\lambda$: Boit number
ω, $\omega^* = L\sqrt{\omega/2\kappa}$: Angular velocity
x, $x^* = x/L$: Depth into wall direction
L : Wall thickness of structure
t : Time
α : Linear expansion coefficient of material
Stuffix * : Non-dimensional number

T_0 : Source fluid temperature difference
T_m^*, T_b^*: Membrane and bending temperature
σ, $\sigma^* = \sigma / \{ E \alpha T_0 / (1-\nu) \}$: Stress
j : imaginative number
κ: Thermal diffusivity of structural material
h : Heat transfer coefficient
λ : Heat conductivity
E : Young's modulus of structural material
ν: Poisson's ratio

1. Introduction

At an incomplete mixing area of high and low temperature fluids in nuclear components, fluid temperature fluctuates with random frequencies. It induces random variations of local temperature gradients in structural walls, which lead to cyclic thermal stresses (Fig.1). When thermal stresses and cycle numbers are large, there are possibilities of crack initiations and propagations. This coupled thermal hydraulic and thermal mechanical phenomenon is called thermal striping, which should be prevented.

After through wall cracks because of the thermal striping phenomenon were found at nuclear plants in service[1][2], large 3D numerical calculations[3] and a modeling based on frequency

transfer function[4] were studied to analyze the reason why these cracks were initiated and penetrated. One of the causes of these through wall cracks is a local thermal spot in a pipe. It is the so-called hot/cold spot problem. By incomplete mixings of fluids, thermal fluctuations are induced locally in a specific spot of the pipe, not in the whole pipe. The local temperature difference between inside and outside this thermal spot induces a local constraint of thermal deformation. Therefore even with the same thermal condition, local thermal fluctuations induce larger stress than the thermal fluctuations in the whole pipe.

This study has two purposes. The first is to analyze the 3D thermal distribution appeared in a local thermal spot and to explain the effect of this thermal distribution against fatigue strength. The next is to develop a simplified evaluation method which can quantify the effect of this local thermal spot.

2. Description of thermal striping phenomena and frequency transfer function model[4][5][6]

A wall model subjected to sinusoidal fluctuation of fluid temperature can explain qualitative response characteristics of structures as in Fig.2. If a frequency of fluctuation is very low, whole temperature of the wall can respond to fluid temperature because thermal diffusivity homogenizes structural temperature. Therefore, low frequency fluctuations do not induce large thermal stress that is caused from temperature gradients in structures. On the other hands, a wall surface cannot respond to very high frequency fluctuation, since a structure has a finite time constant of thermal response. High frequency fluctuations do not lead to large thermal stress. In brief, the magnitude of stress induced by the thermal striping depends on the frequency of the fluctuations.

Fig.3 is a general model to explain a transfer process from fluid temperatures to thermal stress. Fluid temperature T_f^* turns to surface temperature $T_s^*(0)$ through a heat transfer coefficient h. Surface temperature conducts into a structural wall and generates temperature distribution $T_s^*(x^*)$ in structures. Temperature distribution causes thermal stress $\sigma^*(x^*)$, since thermal expansion deformation is constrained.

In order to quantify this mechanism with frequency characteristics, frequency transfer functions formulate the process from fluid temperature to thermal stress. The detailed formulation is in the references[4][5][6], here only formulated results are introduced.

Input of a function is non-dimensional fluid temperature on frequency domain:

$$T_f^*(j\omega) = T_f(j\omega)/T_0 = \Im[T_f(t)/T_0] \tag{1}$$

Through the effective heat transfer function H, fluid temperature turns to surface temperature:

$$T_s^*(0, Bi, j\omega) = H(Bi, j\omega)T_f^*(j\omega) \tag{2}$$

The effective thermal stress function S converts surface temperature to non-dimensional thermal stress as

$$\sigma^*(x^*, Bi, j\omega, R_m, R_b) = H(Bi, j\omega)\, S(x^*, j\omega, R_m, R_b) T_f^*(j\omega)$$
$$= G(x^*, Bi, j\omega, R_m, R_b) T_f^*(j\omega) \quad (3)$$

By inverse Fourier transfer and dimensional factors, we can get time histories of thermal stress.

$$\sigma(x, h, t, R_m, R_b) = \frac{E\alpha T_0}{1-\nu}\, \Im^{-1}[\sigma^*(x^*, Bi, j\omega, R_m, R_b)] \quad (4)$$

The effective heat transfer function H, the effective thermal stress function S, and the frequency transfer function G are calculated as Fig. 4, Fig.5, and Fig.6 [4][5][6].

3. Description of 3D thermal distribution in the partially cooled pipes

Under 3D thermal distribution as Fig.7, there are two types of temperature difference. One is the local temperature gradient in the wall as same as the 1D thermal distribution, and the other is global temperature difference in the plane. For 3D thermal distribution we must consider these two temperature differences. The frequency transfer function model formulates these temperature effects using the constraint efficiency factors as introduced in chapter 4.

To understand the effect of 3D thermal distribution, simplified example FEA models as in Fig.8 were analyzed. The 3D distribution model in Fig.8 is the partially cooled pipe whose colored part is a cold spot. The length of the pipe is 360mm, the external diameter is 166mm, and the thickness is 6.7mm. The initial temperature of the pipe and the surrounding of the pipe are 650℃, and the temperature of injected water is 20℃. The water is cyclically injected to the limited part of the pipe during 15 seconds accompanied by 175 seconds non-injection time. After several cycles of this 190 seconds' cooling and heating, the heat removal by injected water is balanced against the heat input from the surrounding of the pipe. The temperature distribution at this temperature stabilized cycle is obtained by cyclic FEA with the heat transfer coefficient between water and the pipe, and that is 4000[W/m^2/℃]. To compare with the 3D distribution model, 2D and 1D distribution models were calculated with the same thermal transient condition as the 3D distribution. The geometries of the cooled spots are modeled within the limitations of each model. In the 2D model the lower half of the pipe is considered as the thermal spot and in the 1D model the whole pipe is considered as being cyclically cooled.

3.1 Existence of the membrane stress

Fig.9 shows temperature distributions by 3D FEA at 4 seconds after cooling in the temperature stabilized cycle. In the axial cross section, there is temperature distribution along the Z axis. The temperature in the cross section decreases gradually as Z becomes lower, and it is not appeared outside the thermal spot at the same Z, therefore there is membrane stress because of that membrane constraint. In the circumferential cross section, there are also temperature differences along the circumferential direction, and membrane stress because of that membrane constraint.

3.2 Increase of the temperature difference in the thickness

Fig.10 is temperature difference at the axial cross section. The temperature difference in the wall of 3D FEA is larger than the one in the 1D FEA. The temperature profile in the stabilized cycle at inner surface is in Fig.11. The average temperature of the section becomes higher in the 3D FEA due to the higher temperature outside the thermal spot. Due to this higher average temperature, temperature gradient in the 3D FEA becomes higher than the 1D FEA as shown in Fig.12.

3.3 Fatigue lives and crack propagation rates with 3D thermal distribution

Fig.13 and Fig.14 are stress distributions along wall thickness of the pipe models, such as the one along the black arrow in the 3D model at Fig.10. In the 1D results, there are no membrane stresses, however in the 3D results there are membrane stresses, and bending stresses of 3D models are higher than those of 1D's. In the axial direction, there is only one sided constraint but in the circumstantial direction there are both sided constraints, therefore the membrane stress in circumstantial direction is the most increased up to 30% of the total stress.

Fig. 15 shows Von Mises stress profile. The equivalent stress range in the 3D is 653MPa and the one in the 1D is 358MPa. As in Fig.16 this difference brings the difference in estimations of the total strains, the one of 3D is 0.48% and the one of 1D is 0.21%. With using the fatigue resistance curve at 450℃[7], the fatigue life of 3D is estimated as 3.1×10^{4} cycles and the one of 1D is 2.0×10^{7} cycles. Using Paris low, the crack propagation rate of 3D is $1\times10^{-4}\sim1\times10^{-3}$'s order , and the one of 1D is 1×10^{-5}'s order as in Fig.18. As a result, with the estimation of 1D FEA model, the fatigue life is underestimated three orders and the crack penetration cycle is underestimated one order.

4. Constraint efficiency factors to quantify 3D thermal distribution

1D FEA and 3D FEA show different results, and the causes of this are the differences of constraints and average temperatures. The frequency transfer function model uses constraint efficiency factors to express arbitrary constraint conditions. Membrane constraint efficiency factors R_m and bending constraint efficiency factors R_b in the equation (3) are defined as follows.

$$\sigma^*(x^*,Bi,j\omega,R_m,R_b)=(1-R_m)T_m^*+(1-R_b)(1-2x^*)T_b^*-T_s^*(x^*,Bi,j\omega) \quad (5)$$

$0 \le R_m \le 1$, $0 \le R_b \le 1$

$$T_s^*(x^*,Bi,j\omega)=D(x^*,j\omega)\,T_s^*(0,Bi,j\omega)=H(Bi,j\omega)\,D(x^*,j\omega)\,T_f^*(j\omega)$$

$$D(x^*,j\omega)=\frac{T_s^*(x^*,Bi,j\omega)}{T_s^*(0,Bi,j\omega)},\quad D_m(j\omega)=\frac{T_m^*}{T_s^*(0,Bi,j\omega)}=\int_0^1 D(x^*,j\omega)dx^*$$

$$D_b(j\omega)=\frac{T_b^*}{T_s^*(0,Bi,j\omega)}=3\int_0^1 D(x^*,j\omega)(1-2x^*)dx^*$$

where, D: Effective heat conduction function

When these efficiency factors are zero, it arrows free deformation. If these factors are one, it corresponds to a perfectly constraint condition. By using constraint efficiency factors, thermal stress under mixed membrane, bending, and peak constraint conditions, that is 3D thermal distribution, can be expressed as equation (5). For 1D thermal distribution, R_m=0 and R_b=1, therefore there was no difficulty to apply the frequency transfer function model, however for 3D thermal distribution, theses factors must be quantified depending on constraints.

4.1 Definition of the constraint efficiency factors

Magnitudes of thermal expansion strains are different between inside and outside of a thermal spot, because average temperatures are different. In this condition, there is a strain constraint because a thermal deformation can not release this difference of the thermal expansion strains. An efficiency of constraint depends on geometries of a structure and a thermal spot, and is defined as a ratio between stress of an actual structure and stress in the perfectly constrained condition.

Stress induced by a constraint is classified into membrane, bending, and peak components. The constraint efficiency factor as an efficiency of constraint is defined for each stress components. However peak stress is not released by a thermal deformation and is always in the perfectly constrained condition, therefore only the membrane constraint efficiency factor and the bending constraint efficiency factor are effective.

The membrane constraint efficiency factor is a constraint efficiency factor against a membrane stress component. This expresses a constraint induced by difference of thermal expansion membrane strains between inside and outside of a thermal spot.

The bending constraint efficiency factor is a constraint efficiency factor against a bending stress component. This expresses a constraint induced by difference of bending stresses between inside and outside of a thermal spot.

4.2 Constraint efficiency factor of membrane stress

Fig.19 shows a graphical explanation of membrane constraint efficiency factor. ① is the membrane free condition, and ③ is the perfectly constraint condition. The temperature distributions of these are determined with heat transfer phenomena.

② is the circumferential cross section of the actual structure. After cyclic thermal calculations, the temperature distribution of the section is obtained. With this temperature distribution, the average temperatures of the evaluation sections are obtained. In this process the cyclic FEA calculation is inevitable and the cause of the cyclic calculation is heat transfer between injected water and the pipe. Therefore this factor can be calculated more easily by the calculation without heat transfer phenomena.

④,⑤,⑥ in Fig.19 are the conditions without heat transfers. ⑤ corresponds to the same structure which has the same geometry's thermal spot. To calculate the membrane constraint efficiency factor, the minimum temperature of the fluid fluctuation is considered as the average temperature inside the thermal spot, and the maximum temperature of the fluid fluctuation is

considered as the average temperature outside the thermal spot. Comparing the stress in this condition to the stress in the perfectly constrained condition with the same temperature condition, the membrane constraint efficiency factor for this structure can be calculated. This membrane constraint efficiency factor can apply to the same geometry's structure with the same geometry's thermal spot under different temperature conditions. By applying this factor to the perfectly constrained condition of ③, the actual membrane stress can be calculated.

4.3 Constraint efficiency factor of bending stress

Fig.20 shows a graphical explanation of bending constraint efficiency factor. ① is the bending free condition, and ③ is the perfectly bending constraint condition. ② is the circumferential cross section of the actual structure as same as Fig.19. ④,⑤,⑥ in Fig.20 are the conditions without heat transfers. ⑤ corresponds to the same structure which has the same geometry's thermal spot. To calculate the bending constraint efficiency factor, the whole temperature difference between the maximum and the minimum temperature of the fluid fluctuation is considered as bending components in ⑤. In the perfectly constrained condition, the same temperature difference is considered, and comparing the stress in ⑤ to the stress in the perfectly constrained condition, the bending constraint efficiency factor for this structure can be calculated. This bending constraint efficiency factor can apply to the same geometry's structure with the same geometry's thermal spot under different temperature conditions. By applying this factor to the perfectly constrained condition of ③, the actual bending stress can be calculated.

4.4 Example calculation by the frequency transfer function with constraint efficiency factors

Fig.21 shows the calculation example of thermal stress based on the frequency transfer function with constraint efficiency factors. Cyclic thermal transient conditions inside the pipe are modeled as in Fig.22. To calculate the constraint efficiency factors, the temperature conditions in the walls were determined as in Fig.23. With 1 step stress calculation, the constraint efficiency factors for this case are obtained as in Fig.23. Fig.24 shows the calculation results, the horizontal axis is the frequency of the thermal fluctuation in Fig.22, and the vertical axis is the gain against the stress in the perfectly constraint condition. As in Fig.24 the results obtained by the frequency transfer function model with those factors correspond to the results obtained by FEA in all frequency range.

5. Further study plan to standardize the constraint efficiency factor

In the chapter 4, the constraint efficiency factors are defined. To use these factors in the structural designs, further studies are planned.

- Parametric verification by comparisons between the frequency transfer function model with the constraint efficiency factors and full steps of FEA
  +Verifications with different temperature conditions
  +Supplementation of the samples with different geometries
  (The angle of the hot/cold spot, r/t)

- Standardization of the calculation examples
  +Mapping of the calculated examples
  (The angle of the hot/cold spot, r/t, Heat transfer coefficient, Temperature fluctuation range of the spot)
  +Simplified evaluation equations of the constraint efficiency factors based on the mechanism

6. Conclusion

The effects of 3D thermal distributions in partially cooled pipes on fatigue strength were investigated. This 3D effects are summarized into two main features. The one is the generation of the membrane stress because of the membrane constraint. The other is the increase of the temperature difference in the wall which brings larger bending stress than the stress calculated with 1D thermal distribution. These features shorten fatigue lives and accelerate crack propagation rates. In the example case based on 1D and 3D FEA, the fatigue life evaluated by 1D model is underestimated three orders and the crack penetration rate is underestimated one order without consideration of 3D effect.

To quantify the characteristic of 3D thermal distributions, the constraint efficiency factors were introduced into the frequency transfer function model. These factors can be calculated by only 1 step FEA calculations with simplified temperature conditions, and can be applied to arbitrary geometries without any difficulties. Compared with the full steps of FEA results, the stress calculated by the frequency transfer function model with the constraint efficiency factors were validated.

References

[1] Gelineau,O., et al., High cycle thermal fatigue: experience and state of the art in French LMFRs, SMiRT16, Paper#1311, (2001)
[2] Stephan, J.M., et al., Evaluation of the risk of damages in mixing zones: EDF R&D Programme, ASME, PVP-Vol.443-1, pp33/38, (2002)
[3] C. Gourdin, et al., A hydro-thermo-mechanics analyze of the thermal fatigue in the mixing tee junction, SNA-2003, (2003)
[4] Naoto Kasahara, et al., Structural response function approach for evaluation of thermal striping phenomena, Nuc. Eng. Des., 212, pp281/292, (2002)
[5] Naoto Kasahara, et al., Stress response functions to multi-dimensional spatial fluctuations of fluid temperature, ASME, PVP-Vol.443-1, pp25/31, (2002)
[6] Naoto Kasahara, et al., Frequency transfer function from fluid temperature fluctuations to stress intensity factors, ASME, PVP DA021, (2003)
[7] Y.Wada, et al., A statistical approach to fatigue life prediction for SUS304, 316, and 321 austenitic stainless steels, ASME PVP-Vol.123, p43-48
[8] CRIEPI, Draft Guideline for Structural Integrity Assessment for Fast Reactor Plant, CRIEPI,(2002),(in Japanese)
[9] Miura N, et al., Development of Flaw Evaluation Guideline for FBR Components, Trans. Int. Conf. SMiRT 15, Vol.5,(1999), pV.137-V.144

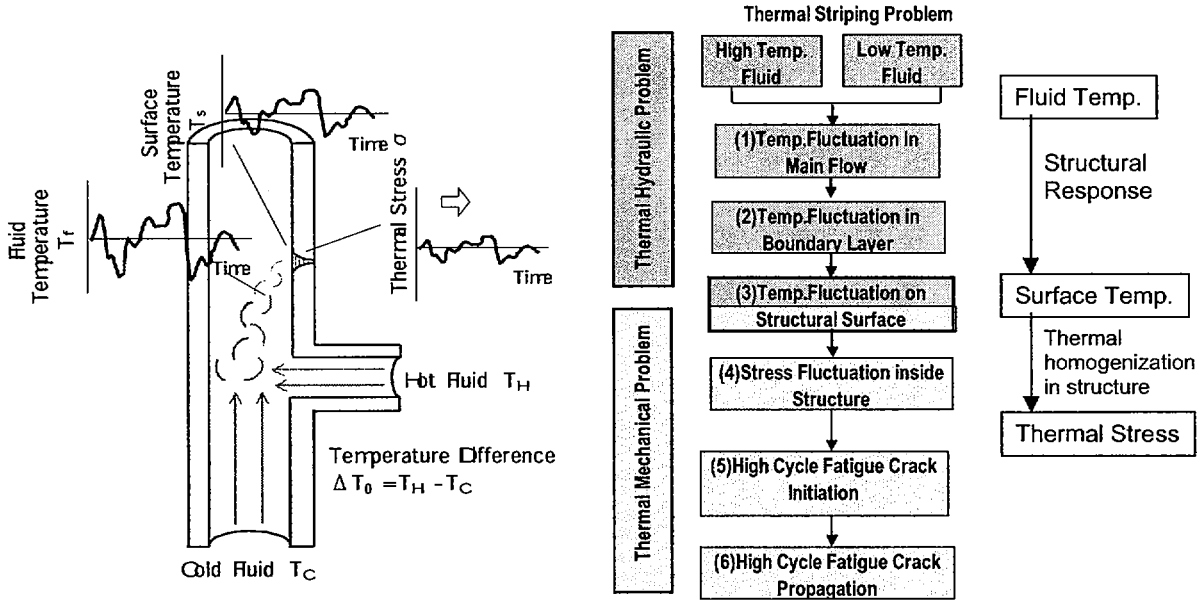

Fig.1 Thermal striping phenomena

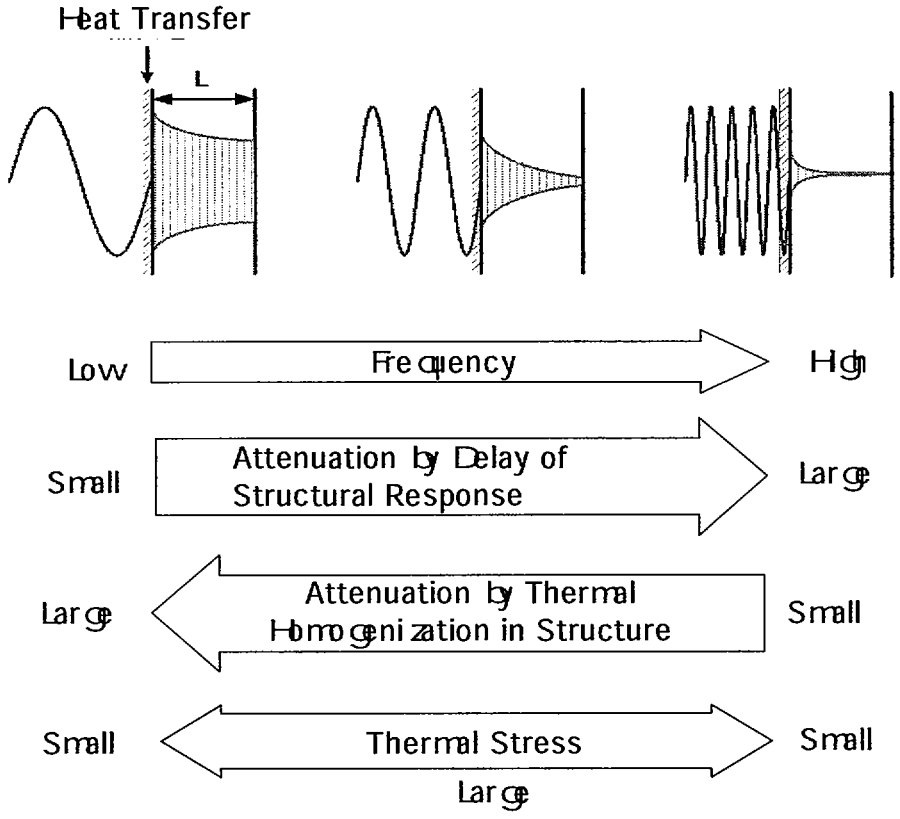

Fig.2 Frequency response characteristics of structural by fluid temperature

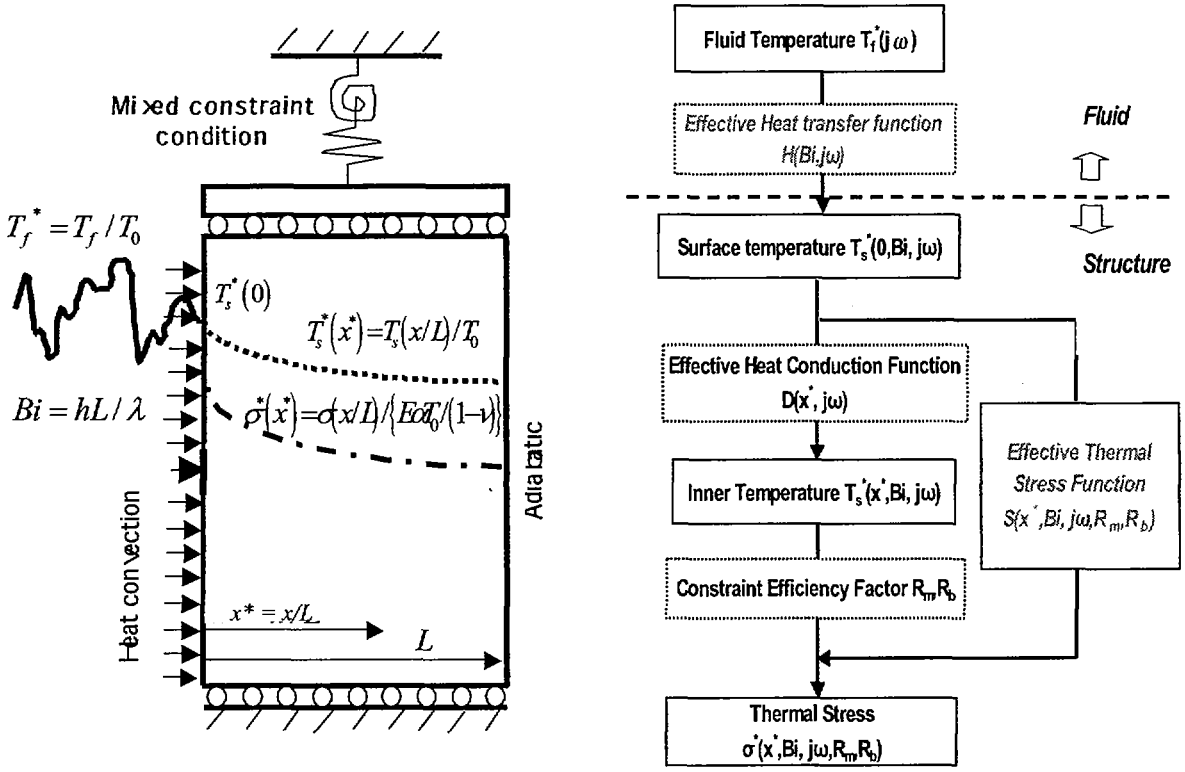

Fig.3 Thermal and mechanical model of structural response by fluid temperature

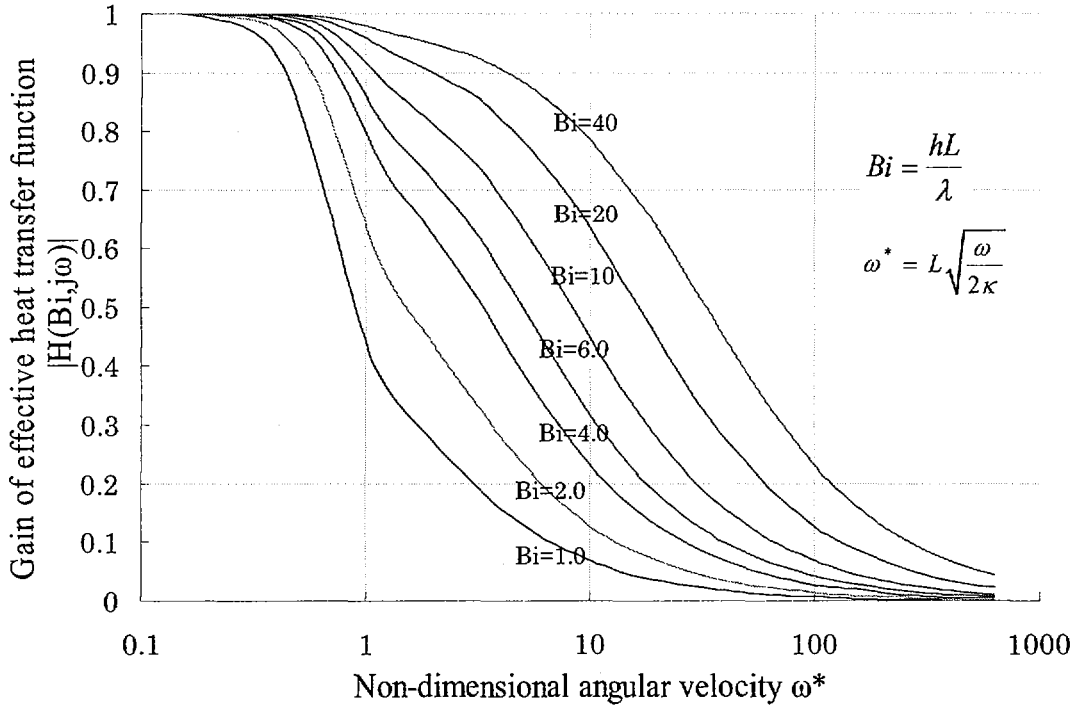

Fig.4 Effective transfer function: H(Bi, jω)

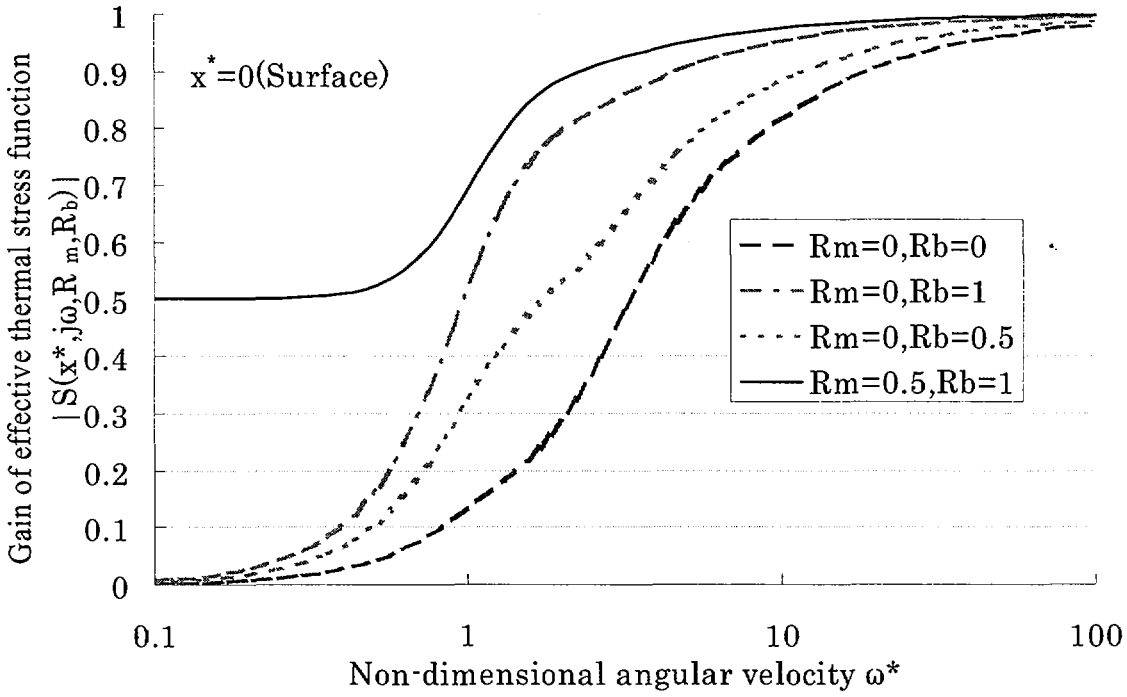

Fig.5 Effective thermal stress function: $S(x^*, j\omega, R_m, R_b)$

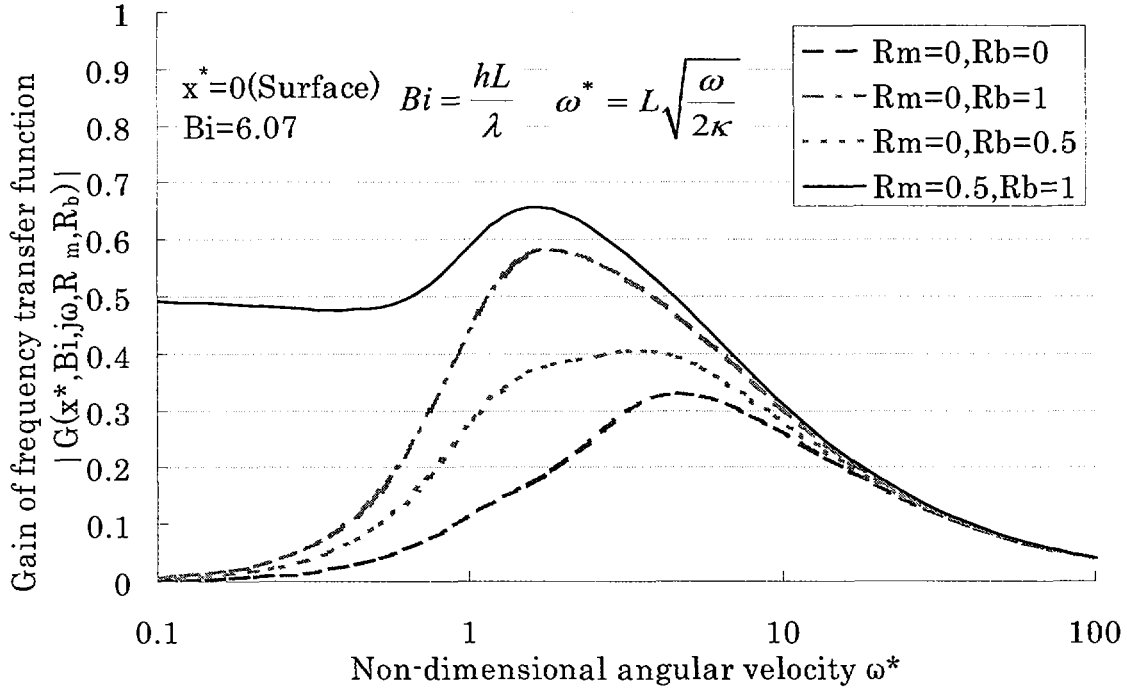

Fig.6 Frequency transfer function: $G(x^*, Bi, j\omega, R_m, R_b)$

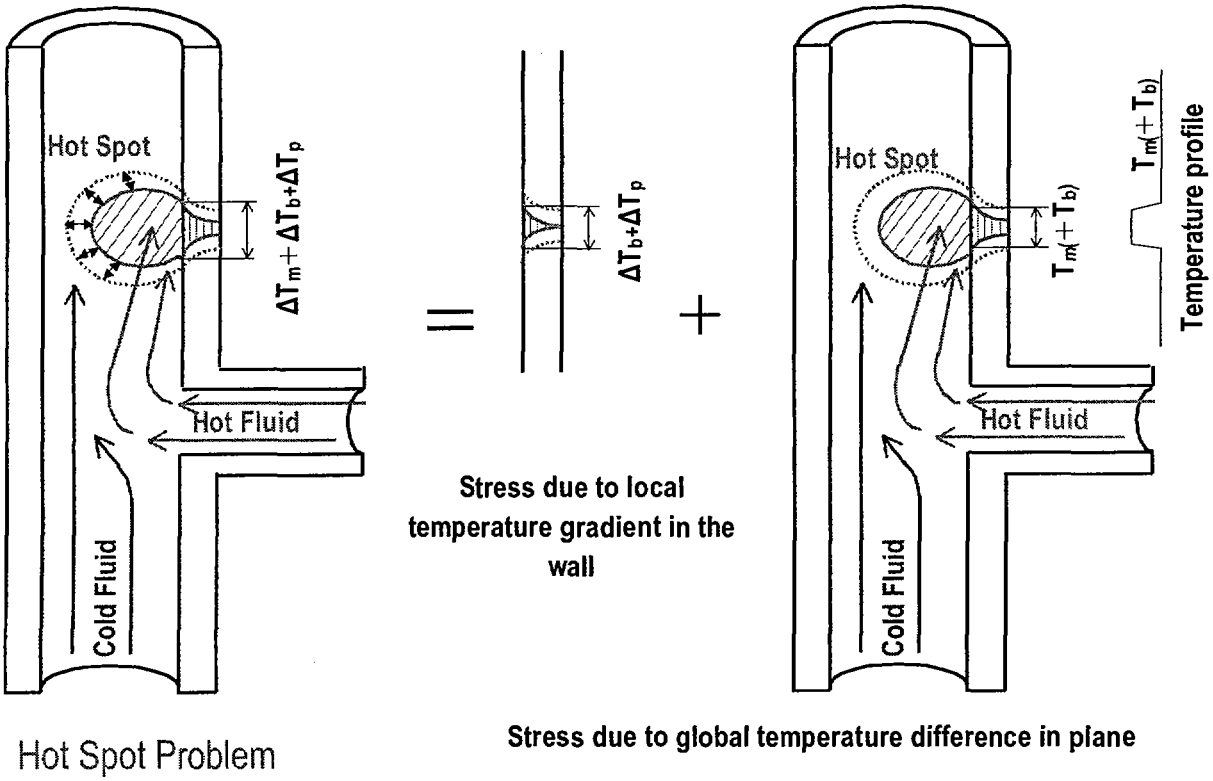

Fig.7 Temperature difference in 3D thermal distribution

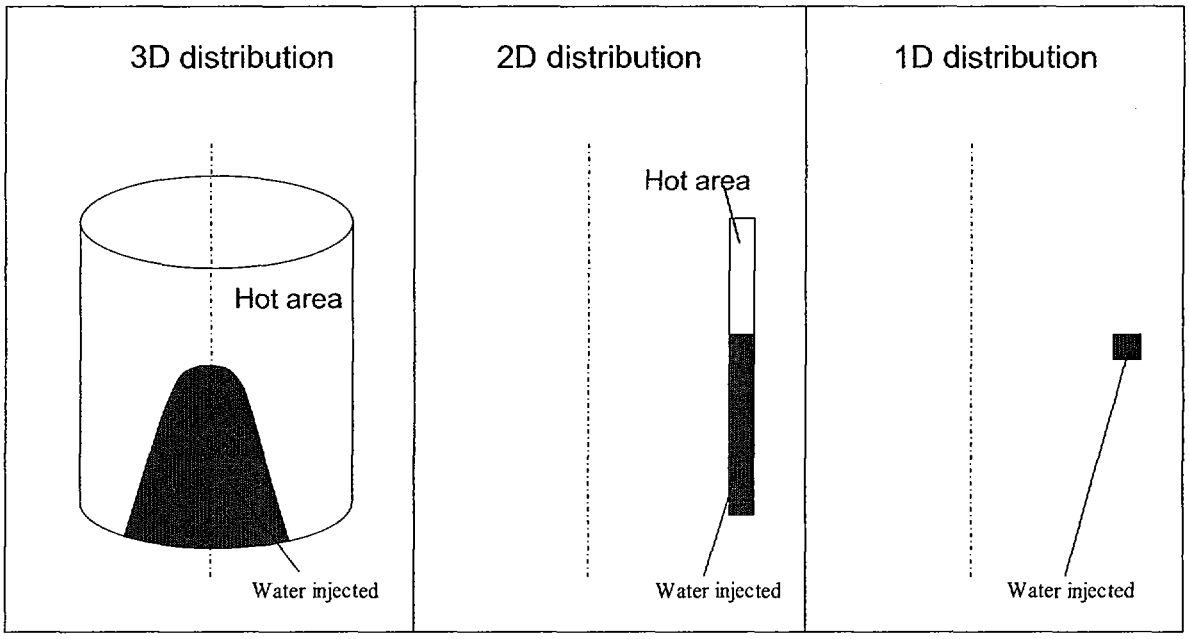

Fig.8 Example of thermal distributions: Cold spot

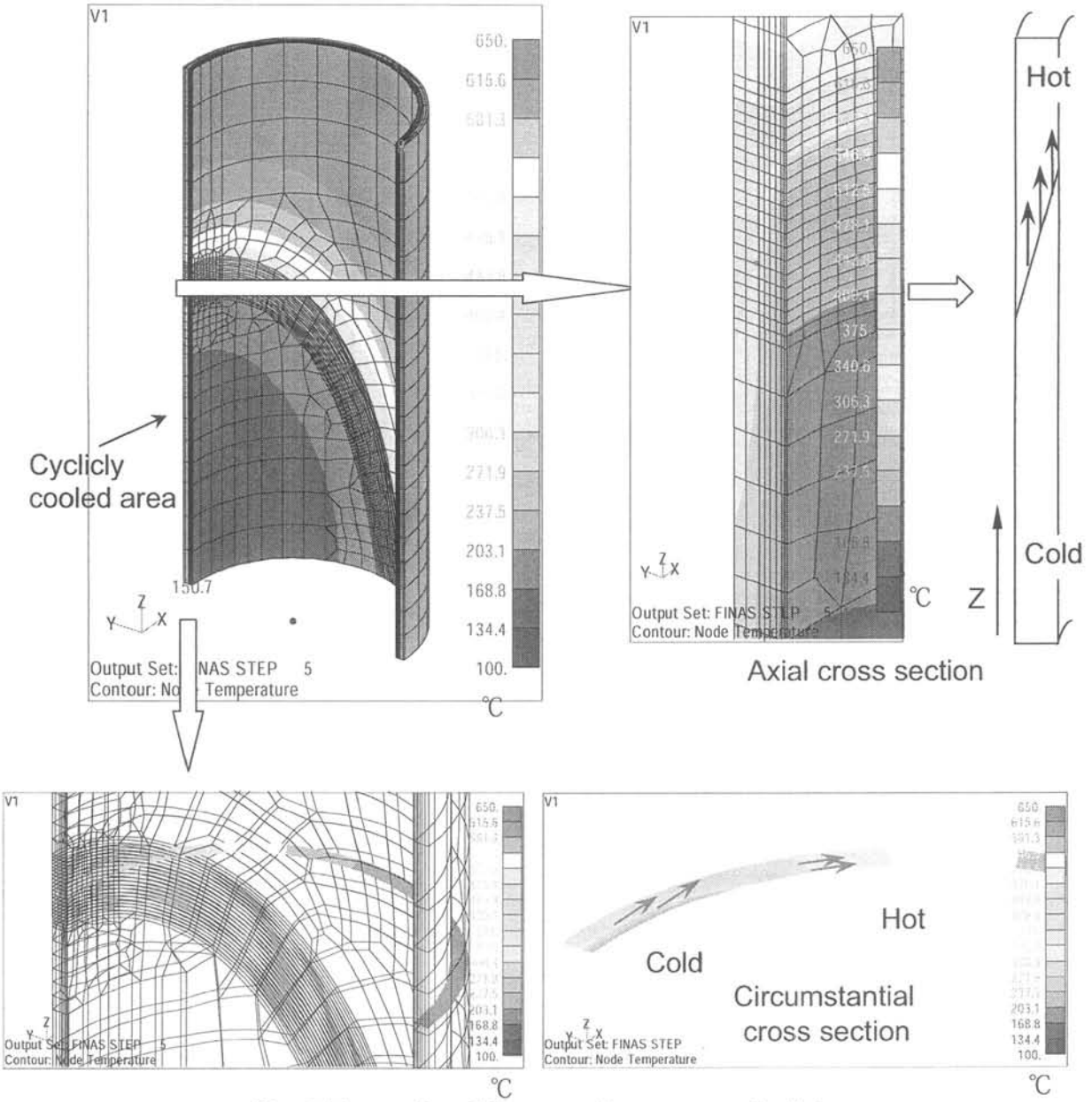

Fig.9 Example of the membrane constraint

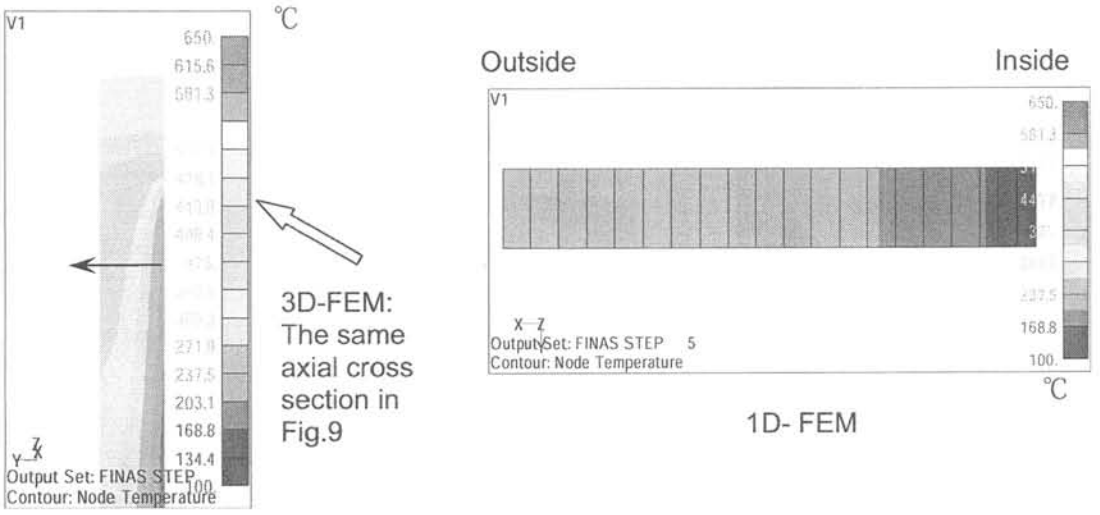

Fig.10 Temperature distribution in the wall at 4 seconds

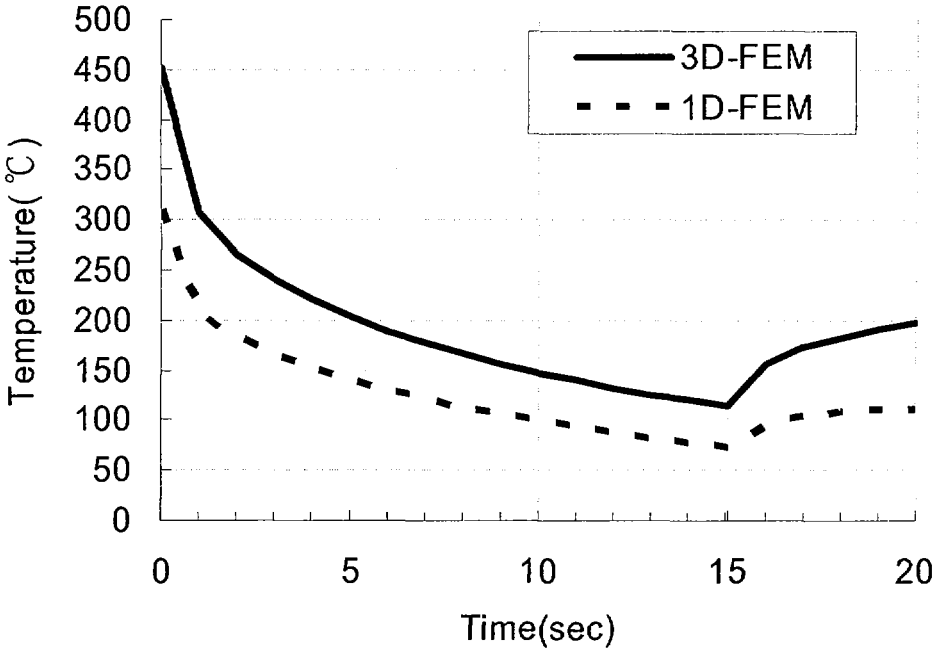

Fig.11 Temperature profile at the inner surface

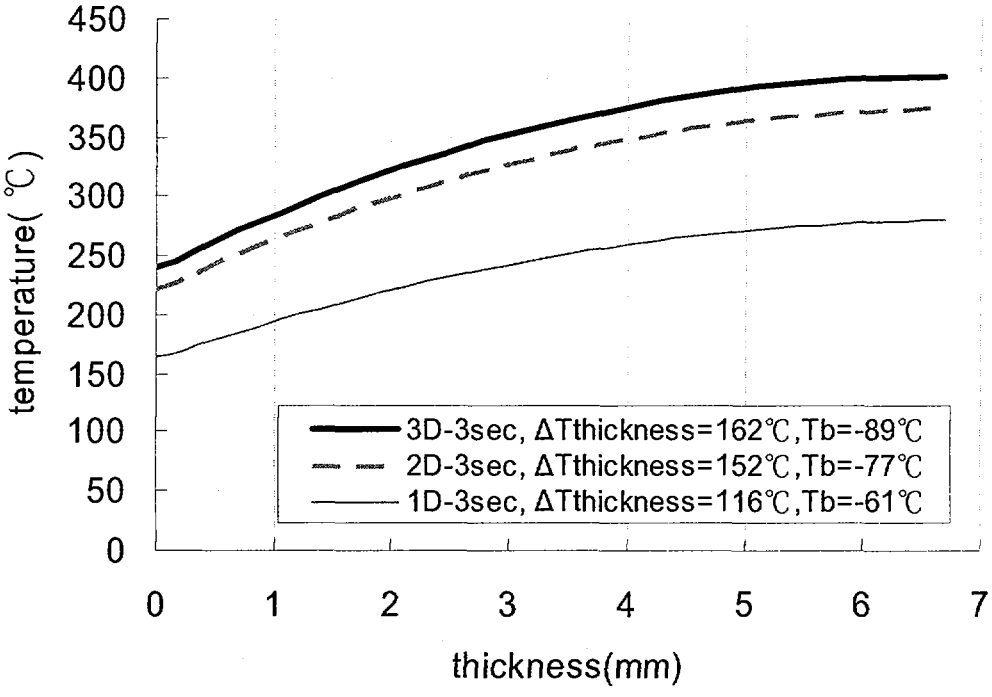

Fig.12 Temperature distribution in the wall - 2

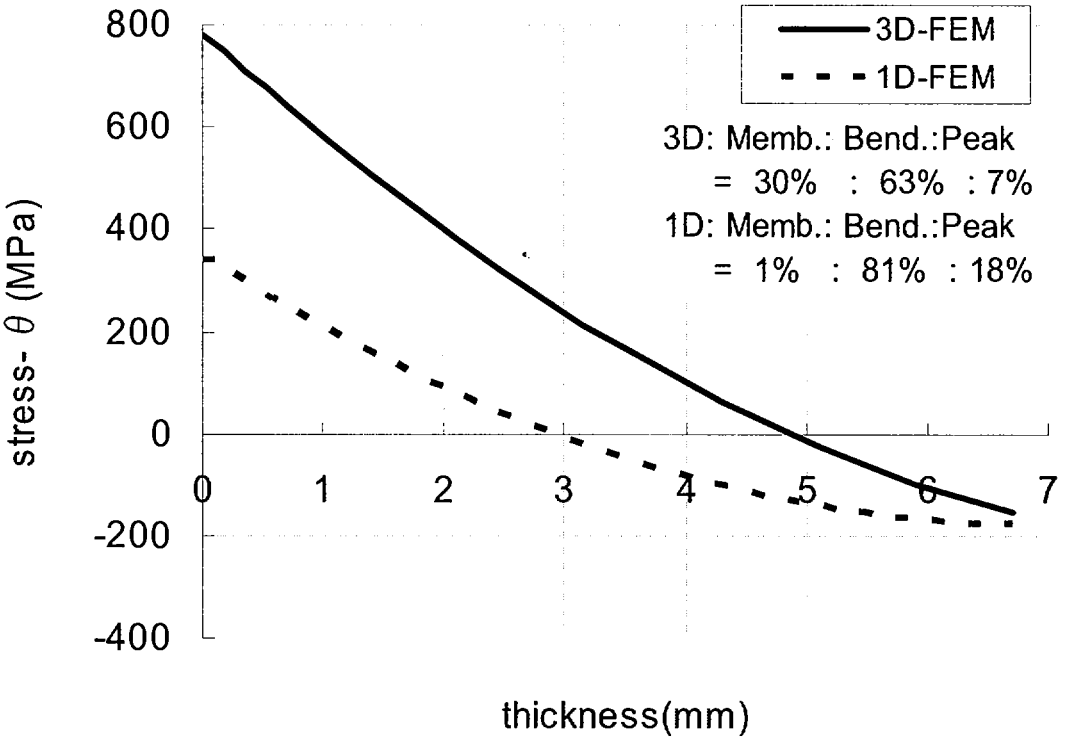

Fig.13 stress distribution in the wall : Circumferential

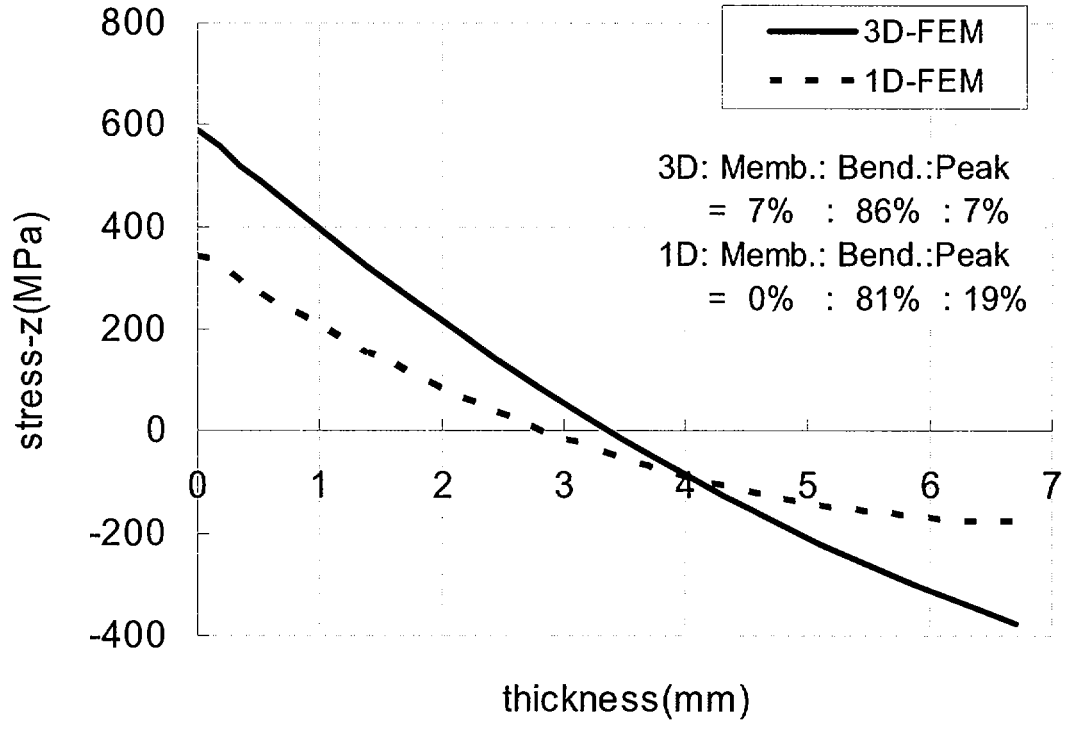

Fig.14 stress distribution in the wall : Axial

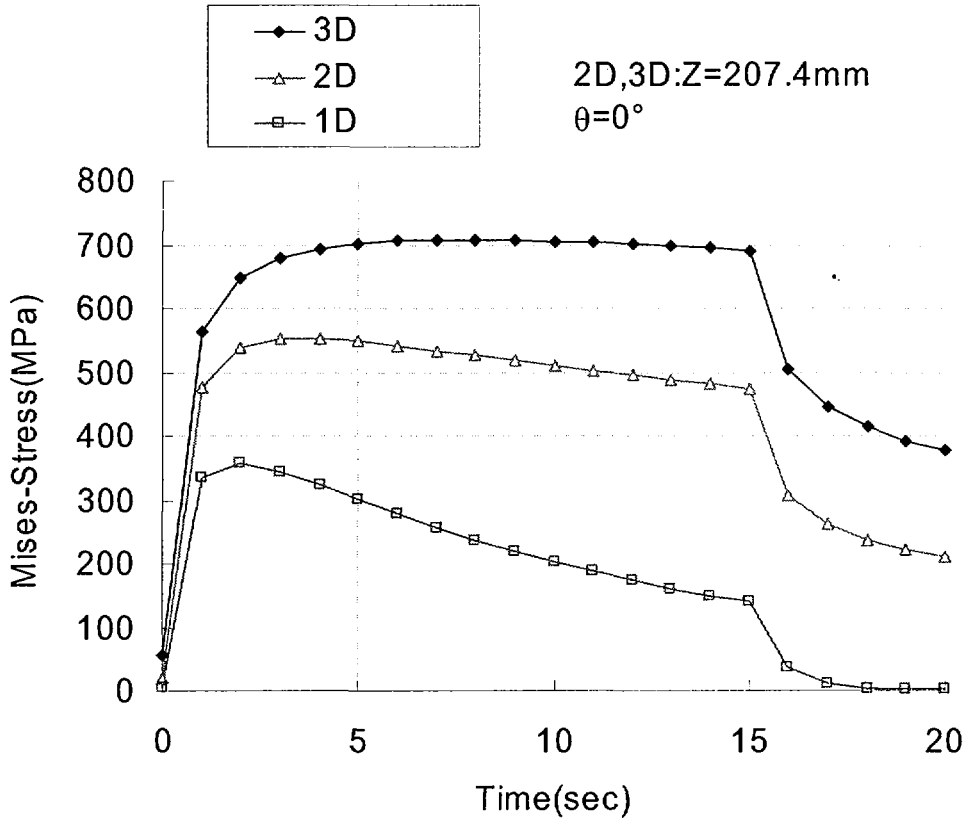

Fig.15 Von Mises stress profile at the inner surface

Case		3D-FEM	1D-FEM
Equivalent stress range	$\Delta\sigma\|_{x=0}$ [MPa]	653	358
Strain consentration factor	Ke'	1.36	1.11
Total strain range	$\Delta\varepsilon_{tot}$ [%]	0.48	0.21
Fatigue life	Nf [cycles]	3.1×10^{4}	2.0×10^{7}
Penetration cycles after initiation	Np [cycles]	10^{3} order	10^{4} order
Crack propagation rate	da/dN [mm/cycle]	$10^{-4}\sim10^{-3}$ order	10^{-5} order

$\Delta\varepsilon_{tot} = Ke'\Delta\varepsilon_e$, $\Delta\varepsilon_e = \Delta\sigma\big|_{x=0} / E$

$Ke' = \{1+(q-1)(1-2\sigma_y / \Delta\sigma\big|_{x=0})\}$

q=5/3

E: Young's modulus
σ_y: Yield stress

$da/dN = 7\times10^{-5}\times\Delta J_f^{1.37}$

$\Delta J_f = F\Delta J_e$, $\Delta J_e = \Delta K^2 / E'$

$\Delta K = K_{max} - K_{min}$, $E' = E/(1-\nu^2)$ [8][9]

F : plastic modification factor
ν: Poisson's coefficient
K: Stress intensity factor

Fig.16 Estimation of fatigue lives and crack propagation rates

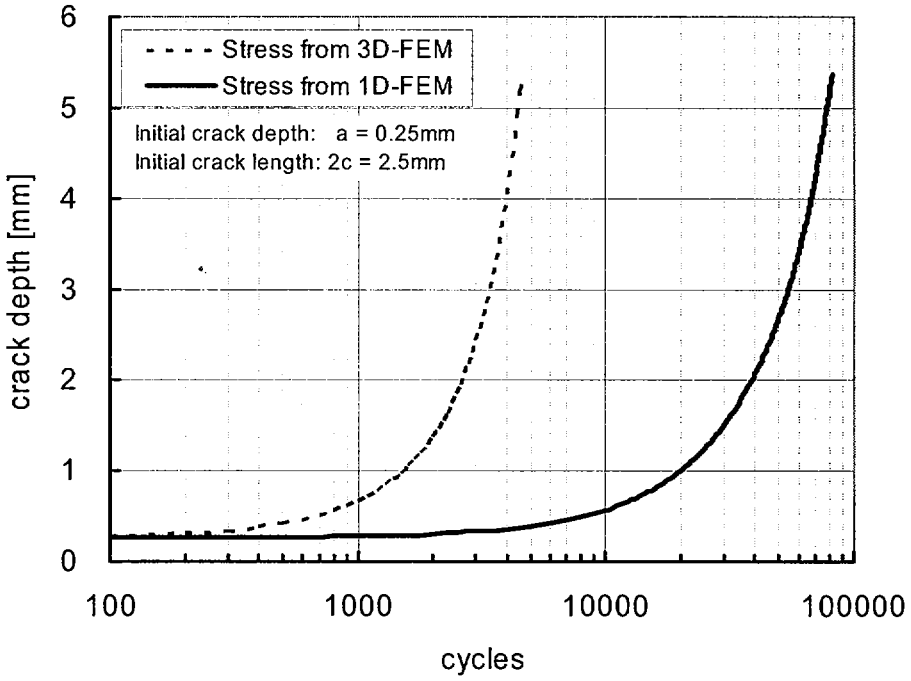

Fig.17 Crack propagation: crack depth

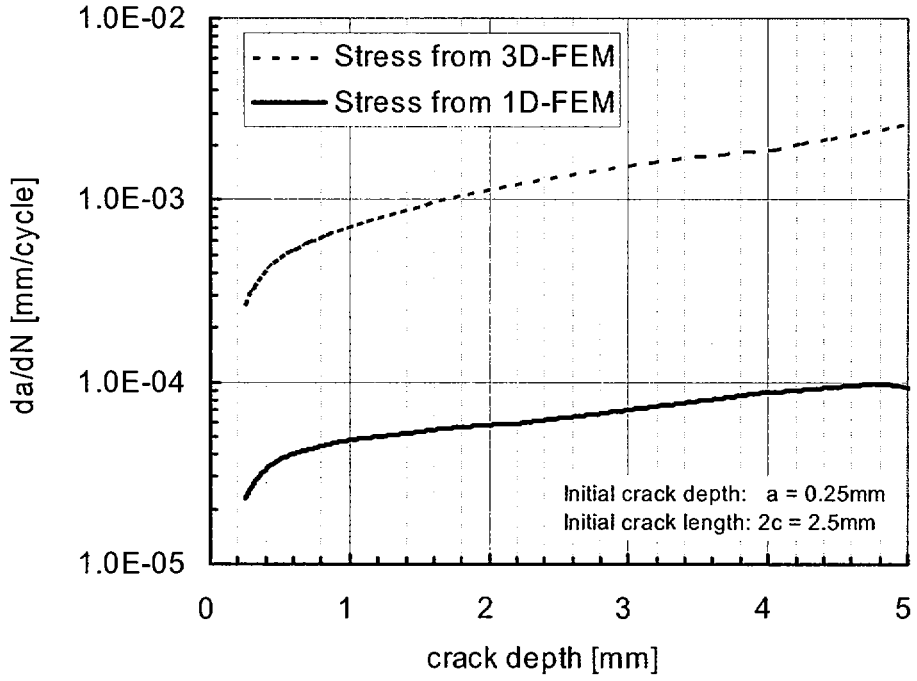

Fig.18 Crack propagation rate

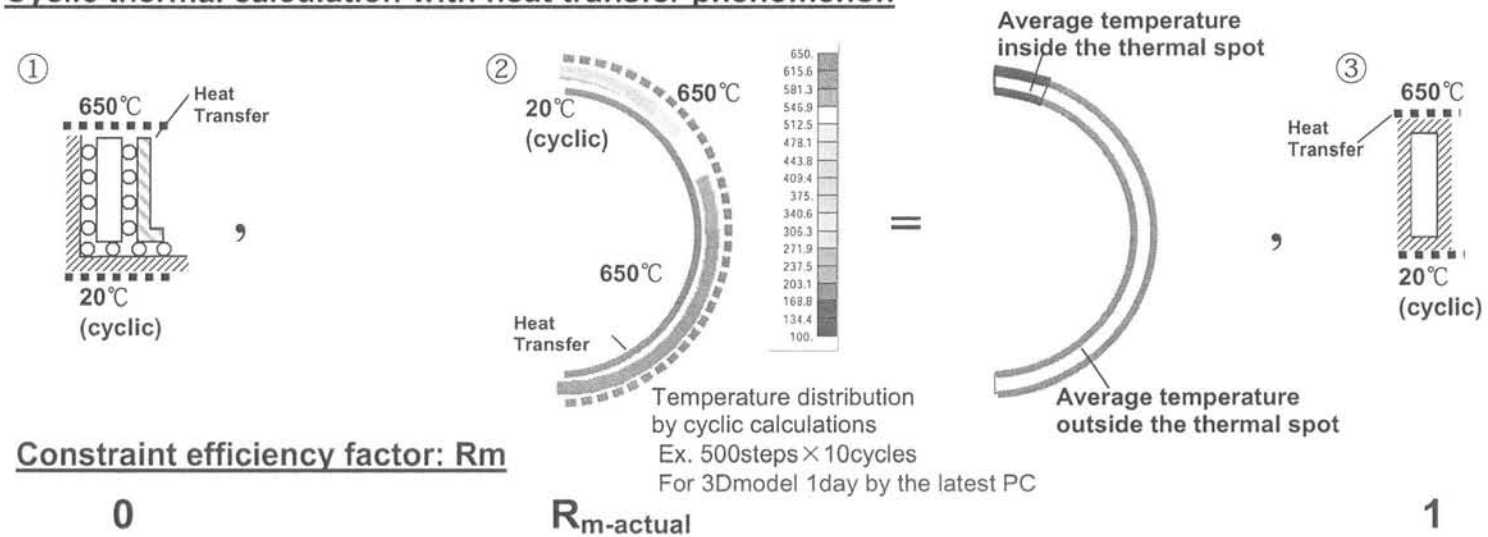

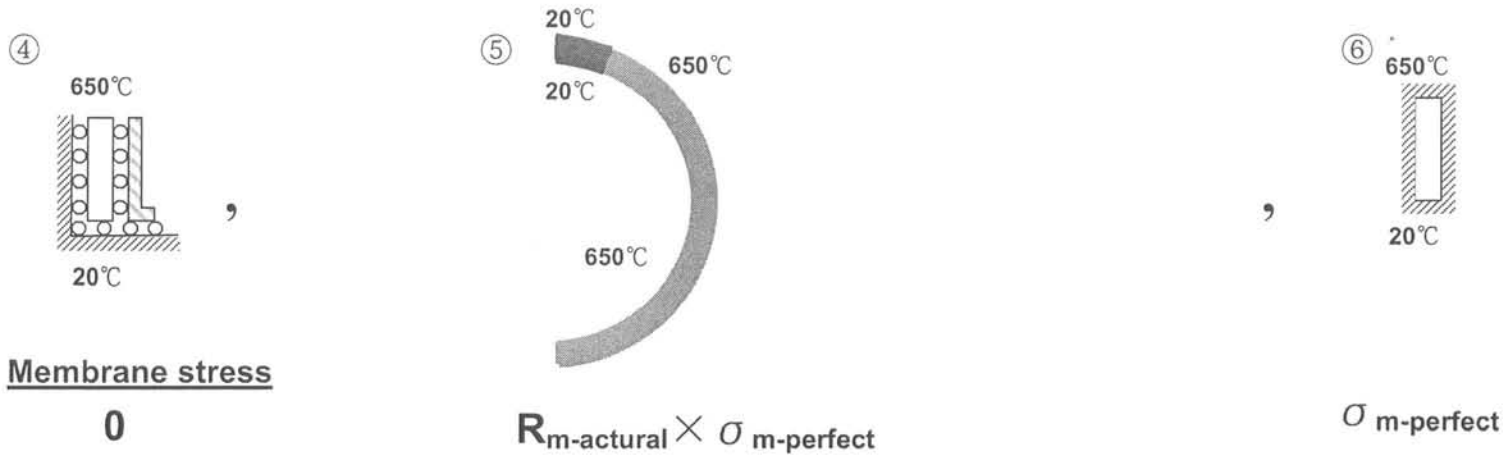

Fig.19 Membrane constraint efficiency factor

Cyclic thermal calculation with heat transfer

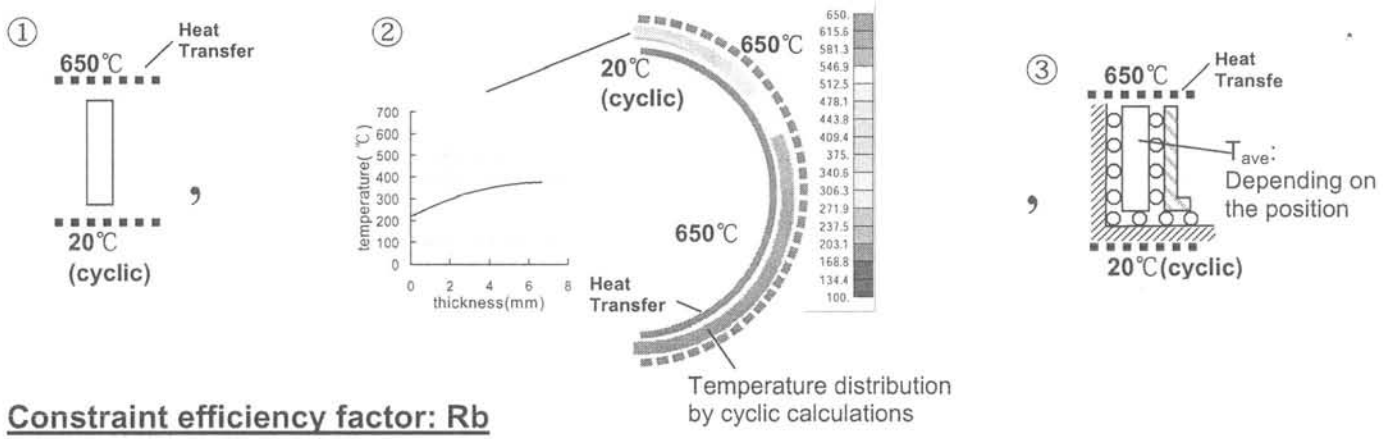

Constraint efficiency factor: Rb

0 $R_{b\text{-actual}}$ **1**

1 step stress calculation with simplified temperature distribution

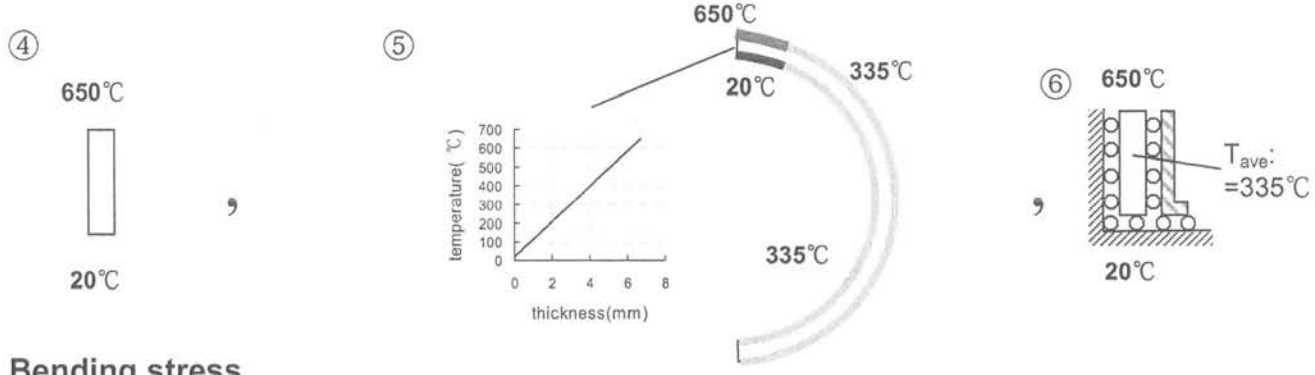

Bending stress

0 $R_{b\text{-actural}} \times \sigma_{b\text{-perfect}}$ $\sigma_{b\text{-perfect}}$

Fig.20 Bending constraint efficiency factor

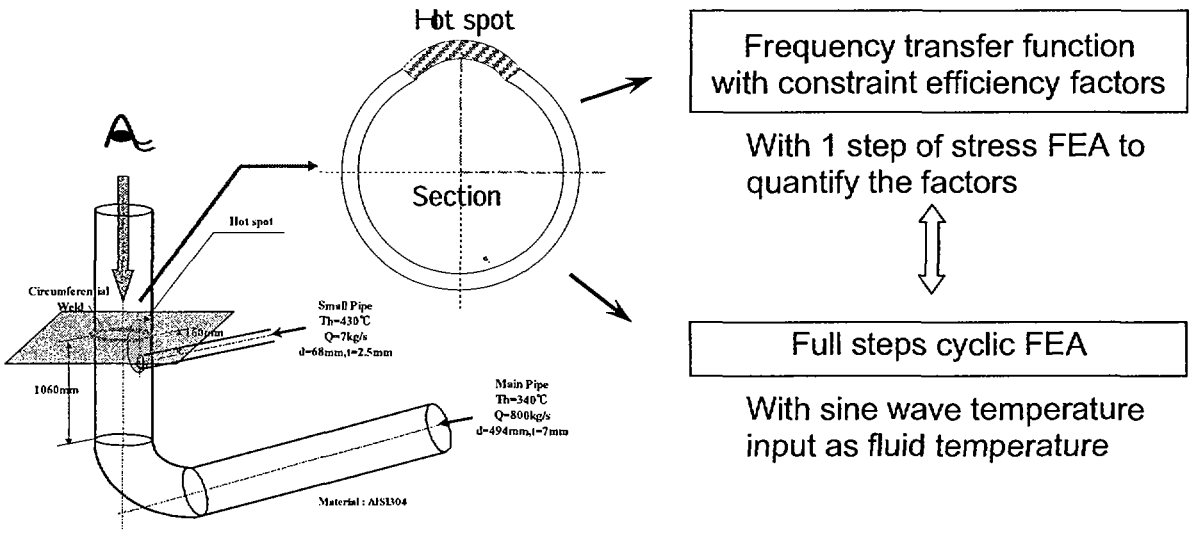

Fig.21 Verification with FEA

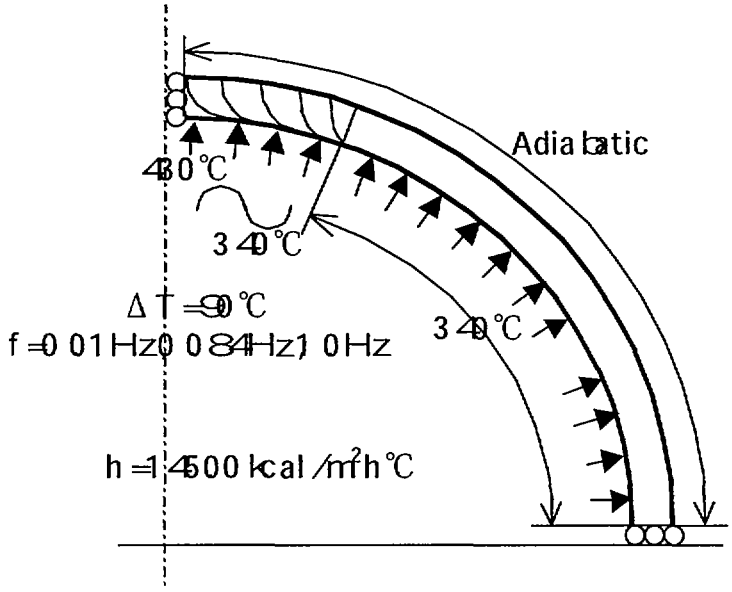

Fig.22 FEA model

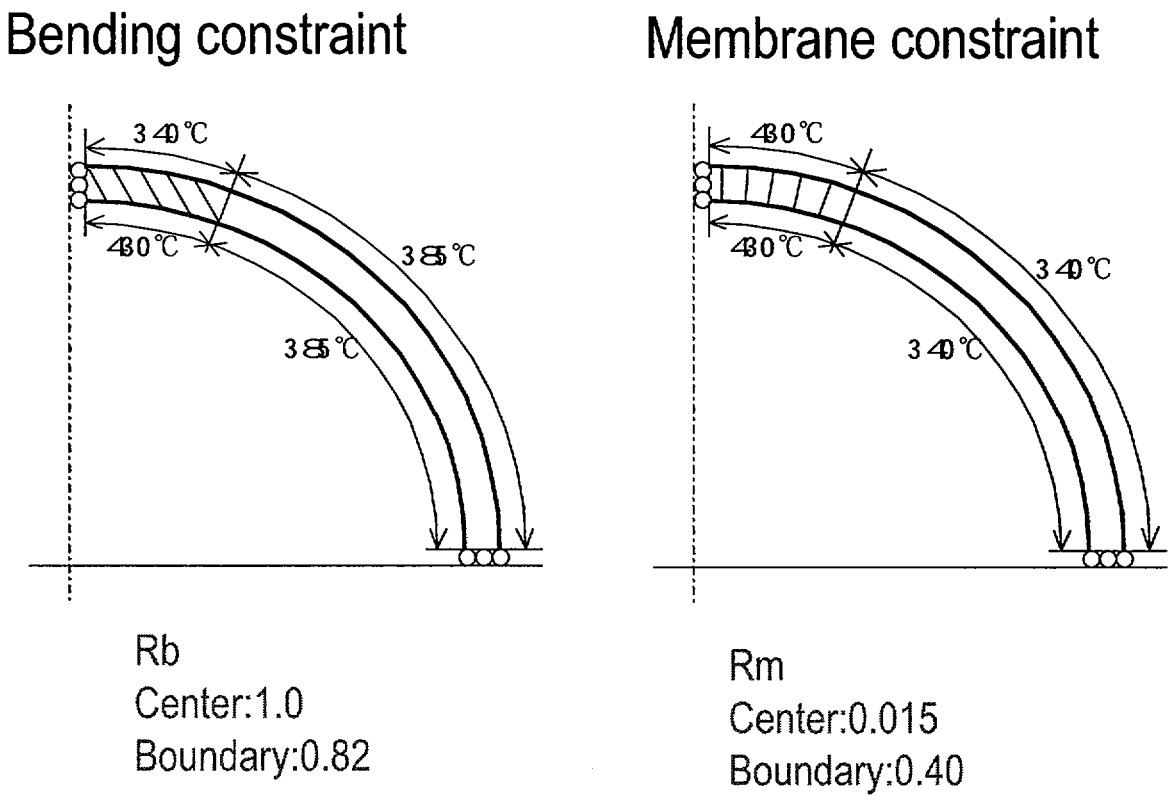

Fig.23 Constraint efficiency factors

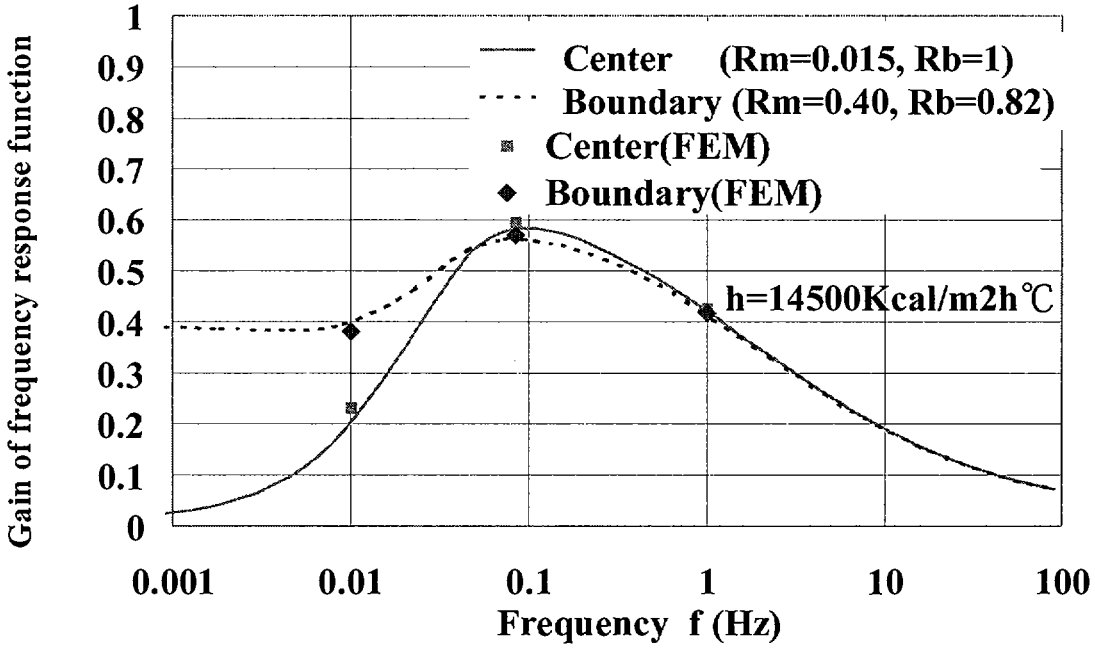

Fig.24 Frequency Transfer Function model and FEA results